CrossMark

ORIGINAL PAPER

Total degradation of *p*-hydroxybenzoic acid by Ru-catalysed wet air oxidation: a model for wastewater treatment

Tijani Hammedi[1] · Mohamed Triki[2] · Mayra G. Alvarez[3] · Ricardo J. Chimentao[3] ·
Zouhaier Ksibi[1] · Abdelhamid Ghorbel[1] · Jordi Llorca[4] · Francisco Medina[3]

Abstract Catalytic wet air oxidation using heterogeneous catalysts is a promising technology for treatment of wastewaters. Wastewaters from olive oil mills are difficult to clean because effluents contain high levels of phenolic compounds that cannot be removed by biological treatment or incineration. Therefore, we tested the catalytic wet air oxidation of *p*-hydroxybenzoic acid, as model molecule of olive oil mills wastewaters, over Ru-supported CeO_2–TiO_2 mixed oxides. We focussed on the Ce/Ti molar ratio because this ratio modifies the properties of the Ru catalysts. Supports were prepared by using the sol–gel method. The Ru catalysts were prepared by impregnation. Those products were characterized by N_2 adsorption–desorption, X-ray diffraction, H_2 chemisorption, transmission electron microscopy and inductively coupled plasma. Catalytic wet air oxidation of *p*-hydroxybenzoic acid was performed in a batch reactor at 140 °C and 50 bar of air. Our results show that the most efficient catalyst was Ru with a Ce/Ti ratio of 1/5, which converted totally *p*-hydroxybenzoic after 7 h of reaction without Ru leaching. We explain this finding by an enhanced dispersion of Ru due to better structural properties of the CeO_2–TiO_2 support.

Introduction

In the last decades, the development of new catalytic oxidation technologies for the removal of organic pollutants has received a great attention. The removal of organic compounds, especially phenolic ones, from wastewaters cannot be achieved by conventional treatments. So, the catalytic wet air oxidation has been assigned an outstanding priority over other wastewater treatment technologies, e.g. photocatalysis (Kanakaraju et al. 2014), electrocoagulation and electro-Fenton (Daghrir and Drogui 2013). It is an attractive method for the treatment of pollutants, which are too diluted to incinerate and too toxic to treat biologically due to their ability to reach mineralization (Cybulski 2007). The use of catalyst makes the process more attractive by achieving high degradation of pollutants at lower temperature and pressure. Moreover, the solid catalyst offers a further advantage, compared to homogeneous catalysis, as the catalyst is easily regenerated and reused (Song and Lu 2015; Bhargava et al. 2007). Noble metals such as Ru and Pt supported on Ti and Zr oxides have been found to be active and stable in catalytic wet air oxidation (Pham et al. 2007; Wang et al. 2008; Mikulová et al. 2007). Previous studies (Oliviero et al. 2001; Renard et al. 2005) have demonstrated that the nature of the material influences the catalytic wet air oxidation of organic compounds. This technology is used as a pretreatment of olive oil mill wastewaters, which are toxic and hardly biodegradable due

✉ Tijani Hammedi
tijanihamm@yahoo.fr

[1] Laboratoire de Chimie des Matériaux et Catalyse, Faculté des Sciences de Tunis, Université Tunis ElManar, Campus Universitaire Tunis ElManar, 2092 Tunis, Tunisia

[2] Laboratoire de Valorisation des Matériaux Utiles, Centre National des Recherches en Sciences des Matériaux, Pôle Technologique Borj Cedria, 8027 Soliman, Tunisia

[3] Departament d'Enginyeria Química, Universitat Rovira i Virgili, Av/Països Catalans 26, 43007 Tarragona, Spain

[4] Institut de Tècniques Energètiques i Centre de Recerca en Nanoenginyeria, Universitat Politècnica de Catalunya, Av. Diagonal, 647, 08028 Barcelona, Spain

to the presence of phenolic pollutants (Pintar et al. 2004; Manole et al. 2007). We used *p*-hydroxybenzoic acid, typically found in olive oil mill wastewaters as model molecule which its physicochemical properties are given in Table 1.

In our previous work, the catalytic wet air oxidation of *p*-hydroxybenzoic acid was conducted in a batch reactor in the presence of ruthenium catalysts supported by CeO_2 mixed oxides, i.e. CeO_2–Al_2O_3 (Triki et al. 2011) and CeO_2–TiO_2 (Triki et al. 2009). These mixed oxides were elaborated via the sol–gel method combined with super-critical drying. This method offers not only a good homogeneity of the different precursors but also the possibility of better controlling of the metal particle size and porosity of the catalyst (Mishra et al. 2004). We have found that doping CeO_2 with an optimum ratio (for the Ce–Al(20) support, 20 is a weight ratio (CeO_2/(CeO_2 + Al_2O_3)) and for Ce–Ti(1/3), 1/3 is a molar ratio (Ce/Ti)) leads to good activity of the supported Ru catalysts in the catalytic wet air oxidation of *p*-hydroxybenzoic acid (Triki et al. 2011). Our results showed that decreasing the Ce/Ti molar ratio from 3 to 1/3 in CeO_2–TiO_2 materials improves the activity of Ru-supported catalysts in the catalytic wet air oxidation of *p*-hydroxybenzoic acid. Nevertheless, CeO_2–TiO_2 seems to be an interesting support worth further exploration. The aim of this work is to study the catalytic properties of Ru/CeO_2–TiO_2 in the catalytic wet air oxidation of *p*-hydroxybenzoic acid batch reactor at 140 °C and 50 bar of air. We thoroughly investigated the effect of the Ce/Ti molar ratio, specific surface area of the supports and the dispersion of metal on the catalytic properties of Ru catalysts.

Materials and methods

Catalyst preparation

CeO_2 was prepared by dissolving $Ce(NO_3)_3{\cdot}6H_2O$ in absolute ethanol. After stirring, droplets of NH_4OH were added to obtain a precipitate. CeO_2–TiO_2 mixed oxides were prepared by the sol–gel method as follows: $Ce(NO_3)_3{\cdot}6H_2O$ was dissolved in absolute ethanol. After the addition of ethylacetoacetate, as chelating agent, titanium(IV) isopropoxide was added in the desired Ce/Ti molar ratio (1/6, 1/5 or 1/4). Hydrolysis was performed with HNO_3 aqueous solution (0.1 M). The obtained gels were dried in supercritical conditions of ethanol ($T = 243$ °C, $P = 63$ bar) and then calcined under oxygen at 500 °C for 3 h. TiO_2 was prepared in the same way but without the addition of cerium nitrate. The 3 wt% Ru catalysts were prepared by impregnation of the support with an ethanolic solution of $Ru(NO)(NO_3)_3$. The mixture was dried at 90 °C for 24 h and then reduced under H_2 at 300 °C for 2 h. The catalysts were labelled as Ru/CeTi(x), where x corresponds to the Ce/Ti molar ratio.

Catalyst characterization

N_2 physisorption at 77 K was carried out in an automatic ASAP 2020 apparatus from Micromeritics. The specific surface area was determined using Brunauer–Emmett–Teller (BET) method, and the average pore diameter was calculated with Barrett–Joyner–Halenda (BJH) method. X-ray diffraction (XRD) measurements were taken using a Philips PW1050 diffractometer with $CuK\alpha$ radiation at $\lambda = 1.5418$ Å. The phases were identified with reference to Joint Committee on Powder Diffraction Standards (JCPDS) cards. The crystallite size of the samples was calculated using the Debye–Scherrer equation:

$$d_{XRD} = \frac{K\lambda}{\beta \cos \theta} \tag{1}$$

where d_{XRD} is the crystallite size (nm), K is the shape factor (0.90), λ is the wavelength (0.154 nm), β is the corrected full width at half maximum (radian), and θ is the Bragg angle (radian). H_2 chemisorption studies were conducted in a Micromeritics ASAP 2010. Before the analysis, the catalyst was reduced in situ (H_2, 300 °C, 2 h). After reduction, the H_2 on the catalyst surface was removed by He (300 °C, 2 h). The sample was subsequently cooled to 36 °C under the same He flow, and hydrogen chemisorption was then performed at the same temperature. Ruthenium dispersion and particle size were determined assuming an H/Ru stoichiometry of 1. Metal dispersion was calculated based on the monolayer coverage of H_2 chemisorption on Ru:

$$D(\%) = \frac{(V_{mon}/22414)}{\text{metal weight}(\%)} \times S \times M \times 100 \tag{2}$$

where V_{mon} is the monolayer coverage of H_2 on Ru (cm³/g STP), 22,414 is the molar volume (mL/mol, STP), S is the stoichiometric factor of H/Ru (S = 1), and M is the atomic mass of Ru (101.07 g/mol). The Ru crystallite size was

Table 1 Physicochemical properties of *p*-hydroxybenzoic acid

Formula	$C_7H_6O_3$
Molecular weight (g/mol)	138.12
Solubility in water at 20 °C (mg/L)	6
Melting point (°C)	216.2
Log pow	1.37
Vapour pressure at 100 °C (Pa)	3.9×10^{-3}

From OECD SIDS Initial Assessment Report for 9th SIAM, France, 1999, UNEP Publications

calculated from the dispersion values assuming the spherical model. Transmission electron microscopy (TEM) images were recorded with a JEOL JEM-1011 electron microscope at 200 kV. The samples were suspended and dispersed by ultrasonic treatment in ethanol. A drop of the fine suspension was placed on a copper TEM grid, which was then loaded into the microscope.

Catalytic wet air oxidation experiments

Catalytic tests were conducted in a Hastelloy C22 batch reactor at 140 °C and a total air pressure of 50 bar with a stirring rate of 1500 rpm. These experiment conditions were previously optimized by Pham et al. (2007). The reactor was loaded with 150 mL of p-hydroxybenzoic acid (CAS N° 99-96-7, Sigma-Aldrich, 99 %) aqueous solution (10 mmol/L; total organic carbon (TOC) = 840 mg/L) and 500 mg of catalyst. After flushing with N_2 to remove air, the reactor was heated to 140 °C under stirring. Then, the stirrer was stopped and pure oxygen was introduced into the reactor until the total pressure reached up to 50 bar. The reaction started when the stirring was switched on. This point was taken as "zero time". Liquid samples were periodically withdrawn from the reactor every 20 min for the first hour and then every hour, and the reaction time was 7 h for all runs. Samples were analysed by means of high-performance liquid chromatography (HPLC, Thermo Finnigan) using a C18 column (Hypersil Gold column 4.6 mm × 250 mm) heated at 40 °C and an ultraviolet detector at 254 nm. The mobile phase was composed by H_2O (Milli-Q), acetonitrile and H_2SO_4 (70/20/10) with a flow rate of 0.7 mL/min. Identifications and quantifications of the aromatic compounds and organic acids were achieved by comparing with standard. Total organic carbon (TOC) was measured with a Shimadzu Model 5050 TOC analyser. Ru leaching and Ce leaching of the catalysts were determined by inductively coupled plasma (ICP) performed on a PerkinElmer Optima 2000 DV ICP apparatus.

Results and discussion

Catalyst characterization

Textural analysis showed that both specific surface areas and average pore diameter of CeO_2–TiO_2 are higher than those of pure TiO_2 and CeO_2. Compared to unmixed TiO_2 and CeO_2, specific surface area increases from 82 to 183 m^2/g for the CeO_2–TiO_2 samples. This result could be due to the modification of the hydrolysis–condensation reaction rates by cerium nitrate (Lopez et al. 2004). Moreover, the textural properties of the CeO_2–TiO_2 mixed oxides depend on the Ce/Ti molar ratio. In fact, the specific

surface area of CeTi(1/5), CeTi(1/6) and CeTi(1/4) was 183, 146 and 125 m^2/g, respectively. The presence of cerium during the formation of the TiO_2 gel had a marked effect on the specific surface area of the mixed solid. This effect has also been observed during the preparation of doped TiO_2 by means of the sol–gel depending on the nature of the doping agent (Gomez et al. 2003). Thus, it is clear that the addition of Ce to TiO_2 causes significant textural changes in the CeO_2–TiO_2 mixed oxides. On the other hand, a slight decrease in the specific surface area was observed after the addition of ruthenium. This could be attributed to some blockage of the porous structure of the support by Ru particles.

X-ray diffraction analysis revealed that for CeO_2, the peaks at $2\theta = 28.6, 33.1, 47.5$ and 56.3° (JCPDS 34-0394) were attributed to cubic CeO_2. For TiO_2, only the anatase phase represented by peaks at $2\theta = 25.2, 37.8, 48.05$ and 53.8° (JCPDS 21-1272) was detected. The CeTi(1/5) sample presents patterns with peaks of both anatase and cubic CeO_2 but broader and weaker than those of pure oxides, indicating a good dispersion of its crystalline phases. In addition, we found that with the introduction of Ce, the crystallite size decreased from 49 to 10, 8 and 40 nm for CeTi(1/6), CeTi(1/5) and CeTi(1/4), respectively, indicating that the Ce species inhibited the growth of anatase crystallites. No diffraction peak of Ru was detected in the patterns of the catalysts, which could indicate the presence of very small particles and/or indicate that the Ru particles are amorphous (Okal et al. 2011).

From the H_2 chemisorption studies, the results showed that the Ru/TiO$_2$ and Ru/CeTi(x) catalysts presented a Ru dispersion of 9.5–32 % and therefore particle sizes of about 3.1–9.4 nm. The Ru dispersion of Ru/CeTi(1/5) was the highest (32 %), which could be due to the high specific surface area of the CeTi(1/5) support.

Transmission electron microscopy images of Ru catalysts are presented in Fig. 1. The images show small Ru particles with uniform dispersion. The Ru/TiO$_2$ and Ru/CeTi(1/5) catalysts presented small crystallite sizes. These results are in agreement with those obtained by H_2 chemisorption and X-ray diffraction.

Catalytic tests

Figure 2 shows the evolution of the p-hydroxybenzoic acid conversion over time in the presence of Ru catalysts. In the absence of the catalyst or in the presence of the support alone, conversion of the p-hydroxybenzoic acid remained below 7 % after 5 h of reaction and then was nearly constant under the operating conditions. With the addition of Ru, the conversion of p-hydroxybenzoic acid was significantly enhanced and high catalytic activity was observed. Our results showed an increase in p-hydroxybenzoic acid
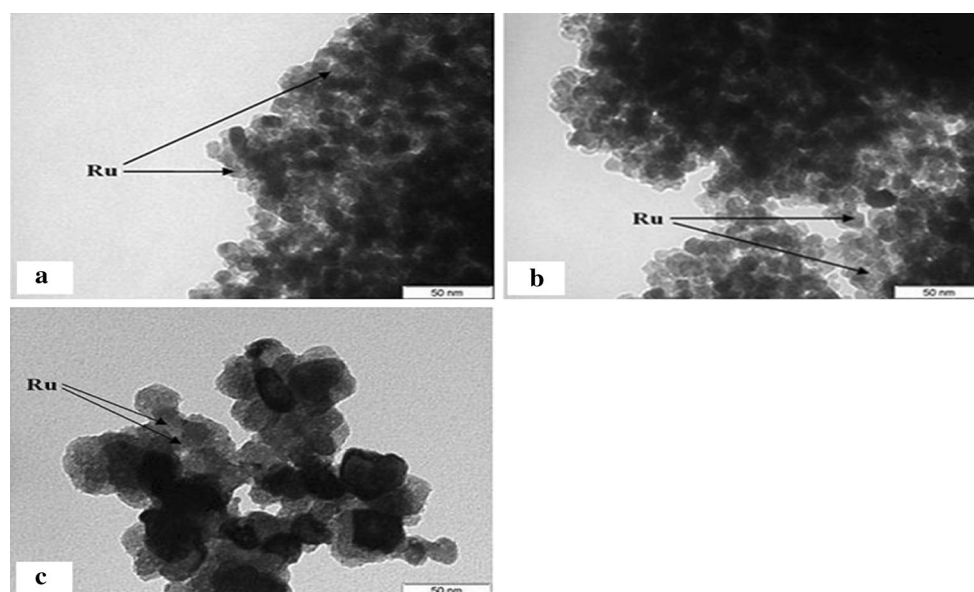
Fig. 1 Transmission electron microscopy images of Ru-supported catalysts. **a** Ru/CeTi(1/5); **b** Ru/TiO$_2$; and **c** Ru/CeO$_2$. The figure shows small Ru particles with uniform dispersion

Fig. 2 *p*-hydroxybenzoic acid conversion in the presence of Ru-supported catalysts (*triangle symbol*) Ru/CeTi(1/5); (*filled square symbol*) Ru/CeTi(1/6); (*times symbol*) Ru/CeTi(1/4); (*circle symbol*) Ru/TiO$_2$; (*diamond symbol*) Ru/CeO$_2$; and (*opened square symbol*) without catalyst. Note the increase in *p*-hydroxybenzoic acid conversion over Ru-supported CeO$_2$–TiO$_2$ mixed oxides comparing to pure oxides. The highest conversion was obtained with an optimum Ce/Ti molar ratio of (1/5)
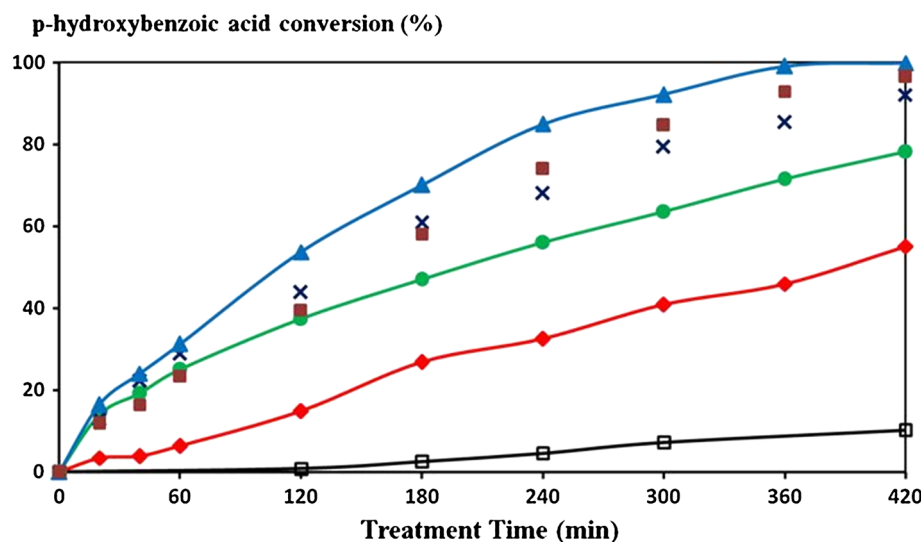
conversion over Ru-supported CeO$_2$–TiO$_2$ mixed oxides comparing to pure oxides. In fact, after 5 h of reaction, the Ru/CeTi(1/6) and Ru/CeTi(1/4) catalysts present higher conversions of *p*-hydroxybenzoic acid (84 and 79 %, respectively) compared to Ru/TiO$_2$ and Ru/CeO$_2$ (63 and 40 %, respectively). Moreover, total conversion of *p*-hydroxybenzoic acid and 93 % of total organic carbon abatement after 7 h of reaction were obtained with the Ru/CeTi(1/5) catalyst.

The activities of the supported Ru catalysts increased as follows: Ru/CeTi(1/5) > Ru/CeTi(1/6) > Ru/CeTi(1/4) > Ru/TiO$_2$ > Ru/CeO$_2$. This order of activity is similar to that observed for the specific surface areas of these different catalysts. Ru/CeTi(1/5) (175 m^2/g) was more active than Ru/

CeTi(1/6) (124 m^2/g), which in turn is more active than Ru/CeTi(1/4) (110 m^2/g). This point is even more evident when correlating the initial reaction rate for the catalytic wet air oxidation reaction based on the specific surface area. Our results showed that the initial activities of the supported Ru catalysts are quite high particularly for Ru/CeTi(1/5) which reaches an initial reaction rate of 0.31 mmol/gmin. The Ru/CeTi(1/5) catalyst is about three times more active than Ru/CeTi(1/4) (0.13 mmol/gmin) and Ru/CeTi(1/6) (0.15 mmol/gmin). The Ru/CeTi(1/4) catalyst, although less active, still exhibits higher activity than the catalyst supported into pure oxide (The initial reaction rates of Ru/TiO$_2$ and Ru/CeO$_2$ were 0.07 and 0.03 mmol/gmin, respectively). A direct correlation can be observed between the enhancement of the textural properties of the mixed oxide

support and catalytic wet air oxidation activity. The increase in catalytic wet air oxidation activities could be ascribed to an increase in the specific surface area of the CeO_2–TiO_2 support, which would enhance the adsorption of oxygen on the catalyst surface. The Ce–Ti system, prepared via the sol–gel method, plays a significant role compared to the corresponding single-oxide system because it permits good CeO_2 dispersion, promotes its electronic properties and so improves the dispersion of the metal (Epron et al. 2002). On the other hand, it seems that the reduction behaviour of Ru on the Ce–Ti system plays a crucial role in the improvement of catalytic activity because the Ru–O–Ce bonds in the well-dispersed Ru particles are highly fragile. The most important intermediates observed during the reaction were phenol, hydroquinone, maleic acid and oxalic acid as previously reported (Triki et al. 2009). Figure 3 presents a simplified reaction scheme describing the formation of the main intermediate compounds during p-hydroxybenzoic acid degradation. This degradation proceeds through decarboxylation to phenol and further hydroxylation of the aromatic ring to yield mainly hydroquinone. The breakdown of the aromatic ring results in the formation of a wide range of cleavage compounds of these; it was possible to detect maleic acid and fumaric acid (by isomerization), CO_2 and water (Pham et al. 2007).

During catalytic wet air oxidation, the active component leaches out from the catalyst, which could cause additional pollution. To investigate the catalyst stability in terms of metal leaching, the concentration of Ru, Ti and Ce ions in the solution after 7 h of reaction was analysed using inductively coupled plasma. We found that no metal leaching of Ce, Ti or Ru (<0.02 mg/L) was detected in any of the treated aqueous solutions, indicating a good stability of Ru catalysts during the catalytic wet air oxidation of p-hydroxybenzoic acid.
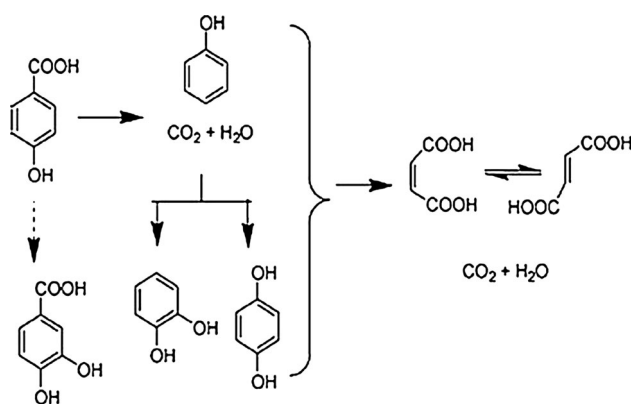

Fig. 3 Simplified reaction scheme of p-hydroxybenzoic acid degradation. The oxidation of p-hydroxybenzoic acid proceeds through decarboxylation to phenol and further hydroxylation of the aromatic ring to yield mainly hydroquinone. Breakdown of the aromatic ring results in the formation of cleavage compounds of these. The formation of maleic and fumaric acids (by isomerization), as well as CO_2 and water, was detected

Conclusion

Ru catalysts supported on CeO_2–TiO_2 aerogel mixed oxides exhibit good activity in the catalytic wet air oxidation of p-hydroxybenzoic acid. Ru/CeTi(1/5) shows the highest activity (100 % of p-hydroxybenzoic acid conversion after 7 h). This molar ratio makes it possible to obtain the highest specific surface area for the support and therefore a better Ru dispersion with small particle sizes. The high catalytic activity is due not only to the high dispersion of Ru particles, but also to the synergy effect between CeO_2 and TiO_2 affecting the structural properties of the CeO_2–TiO_2 support and so permitting an enhancement of O_2 availability to the active sites. Further studies are, however, required to characterize the catalyst after reaction and to optimize the operating conditions under realistic conditions.

References

Bhargava SK, Tardio J, Jani H, Akolekar DB, Foger K, Hoang M (2007) Catalytic wet air oxidation of industrial aqueous streams. Catal Surv Asia 11:70–86

Cybulski A (2007) Catalytic wet air oxidation: are monolithic catalysts and reactors feasible. Ind Eng Chem Res 46:4007–4033

Daghrir R, Drogui P (2013) Coupled electrocoagulation–electro-Fenton for efficient domestic wastewater treatment. Environ Chem Lett 11:151–156

Epron F, Gauthard F, JrJ Barbier (2002) Catalytic reduction of nitrate in water on a monometallic Pd/CeO_2 catalyst. J Catal 206:363–367

Gomez R, Lopez T, Ortiz-Islas E, Navrrete J, Sanchez E, Tzompantzi F, Bokhimi X (2003) Effect of sulfation on the photoactivity of TiO_2 sol–gel derived catalysts. J Mol Catal A 193:217–226

Kanakaraju D, Glass BD, Oelgemoller M (2014) Titanium dioxide photocatalysis for pharmaceutical wastewater treatment. Environ Chem Lett 12:27–47

Lopez T, Rojas F, Katz R, Galindo F, Balankin A, Buljan A (2004) Porosity, structural and fractal study of sol–gel TiO_2–CeO_2 mixed oxides. J Solid State Chem 177:1873–1885

Manole CC, Julcour-Lebigue C, Wilhelm AM, Delmas H (2007) Catalytic oxidation of 4-hydroxybenzoic acid on activated carbon in batch autoclave and fixed-bed reactors. Ind Eng Chem Res 46:8388–8396

Mikulová J, Rossignol S, JrJ Barbier, Mesnard D, Kappenstein C, Duprez D (2007) Ruthenium and platinum catalysts supported on Ce, Zr, Pr–O mixed oxides prepared by soft chemistry for acetic acid wet air oxidation. Appl Catal B 72:1–10

Mishra MK, Tyagi B, Jasra RV (2004) Synthesis and characterization of nano-crystalline sulfated zirconia by sol–gel method. J Mol Catal A 223:61–65

Okal J, Zawadzki M, Tylus W (2011) Microstructure characterization and propane oxidation over supported Ru nanoparticles

synthesized by the microwave-polyol method. Appl Catal B 101:548–559

Oliviero L, Barbier J Jr, Duprez D, Wahyu H, Ponton JW, Metcalfe IS, Mantzavinos D (2001) Wet air oxidation of aqueous solutions of maleic acid over Ru/CeO$_2$ catalysts. Appl Catal B 35:1–12

Pham MD, Aubert G, Gallezot P, Besson M (2007) Degradation of olive oil mill effluents by catalytic wet air oxidation: 2-oxidation of p-hydroxyphenylacetic and p-hydroxybenzoic acids over Pt and Ru supported catalysts. Appl Catal B 73:236–246

Pintar A, Berci G, Besson M, Gallezot P (2004) Catalytic wet air oxidation of industrial effluents: total mineralization of organics and lumped kinetic modeling. Appl Catal B 47:143–152

Renard B, Barbier J Jr, Duprez D, Durécu S (2005) Catalytic wet air oxidation of stearic acid on cerium oxide supported noble metal catalysts. Appl Catal B 55:1–10

Song A, Lu G (2015) Catalytic wet oxidation of aqueous methylamine: comparative study on the catalytic performance of platinum–ruthenium, platinum, and ruthenium catalysts supported on titania. Environ Technol 36:1160–1166

Triki M, Ksibi Z, Ghorbel A, Medina F (2009) Preparation and characterization of CeO$_2$–TiO$_2$ support for Ru catalysts: application in CWAO of p-hydroxybenzoic acid. Micro Meso Mater 117:431–435

Triki M, Ksibi Z, Ghorbel A, Medina F (2011) Preparation and characterization of CeO$_2$–Al$_2$O$_3$ aerogels supported ruthenium for catalytic wet air oxidation of p-hydroxybenzoic acid. J Sol–Gel Sci Technol 59:1–6

Wang J, Zhu W, Yang S, Wang W, Zhou Y (2008) Catalytic wet air oxidation of phenol with pelletized ruthenium catalysts. Appl Catal B 78:30–37